Nuclear Materials and Energy 000 (2016) 1–7

Contents lists available at ScienceDirect

Nuclear Materials and Energy

journal homepage: www.elsevier.com/locate/nme

Quantitatively measuring the influence of helium in plasma-exposed tungsten

R.P. Doerner[a,*], M.J. Baldwin[a], M. Simmonds[a], J.H. Yu[a], L. Buzi[b,1], T. Schwarz-Selinger[c]

[a] Center for Energy Research, UCSD, La Jolla, CA. 92093-0417, USA
[b] Ghent University, Department of Applied Physics, Sint-Pietersnieuwstraat 41, B-9000 Ghent, Belgium
[c] Max-Planck Institut für Plasmaphysik, Boltzmannstrasse 2, D-85748, Garching, Germany

ARTICLE INFO

Article history:
Received 7 June 2016
Revised 23 August 2016
Accepted 7 September 2016
Available online xxx

Keywords:
Plasma-material interactions
Helium
Tungsten
Retention

ABSTRACT

Tungsten samples are exposed to ^{3}He plasma to quantify their helium retention behavior. The retention saturates quickly with helium fluence and increases only slightly from 4.3×10^{19} He/m^2 at 773 K, to 7.5×10^{19} He/m^2 at 973 K. The helium content increases dramatically to 6.8×10^{20} He/m^2 when fuzz is formed on the surface of a sample exposed at 1173 K, but the majority of the retained helium (5.1×10^{20} He/m^2) is found to reside below the layer of fuzz tendrils. Additional tungsten samples were exposed to either simultaneous, or sequential, D/He plasma, followed by TDS. Measurements show the majority of the D retained during simultaneous exposures is located in the near surface region of helium nano-bubbles. No deuterium was detected in any of the samples after the heating to 1273 K, but 67% of the helium was released from simultaneously exposed samples, and only 23% of the helium was released from the sequentially exposed samples.

1. Introduction

During any burning D/T plasma scenario helium ash will be included in the flux of particles striking the plasma-facing materials; both the divertor surfaces as well as the first wall. The exposure of tungsten to energetic (above approximately 30 eV [1]) helium particles results in the formation of a variety of nano-scale surface structures. At surface temperatures below ~1000 K, a dense array of nano-bubbles forms in the uppermost 20–30 nm of the surface [2,3], at temperatures between ~1000 K and ~2000 K tungsten fuzz [4,5] is observed to grow out from the surface and at higher temperature the fuzz disappears leaving an array of larger scale (micron size) pits in the surface [6,7]. While a large amount of experimental research has gone into investigating the behavior of helium in tungsten, much of the work has been observational and qualitative. An equally large effort has gone into modeling the behavior of helium and hydrogenic isotopes in a tungsten lattice [8–10 and references therein] in an attempt to gain insight into the experimental observations. This modeling effort has unfortunately been somewhat hampered by the lack of quantified properties of the helium and deuterium remaining in the tungsten against which to compare results. In this paper, measurements of the amount of helium and deuterium contained in plasma-exposed tungsten are presented under a variety of plasma exposure conditions. Each experiment described has been developed with the aim of testing a specific prediction that emanates from the modeling.

2. Experimental approach

Pure deuterium, or helium, plasma and mixtures of D/He containing plasma are created in the PISCES-A linear plasma device [11] for each different exposure case. In the mixed D/He plasma exposures, the tungsten grade used was chosen according to the specifications approved for ITER material selection [12] supplied by Negele Hartmetall-Technik GmbH. Tungsten rods of 99.94 wt% purity were manufactured with grains elongated parallel to the length of the rod to insure better heat transport and inhibit delamination. Samples were cut perpendicular to the tungsten rod with 4 mm thickness and fabricated with a 'top-hat' shape where the plasma-exposed surface was 14 mm in diameter. Prior to the plasma exposure, samples were mechanically polished to a mirror finish and annealed at 1273 K for one hour.

In the case of the mixed plasma, the helium ion content of the plasma is measured spectroscopically, as described in [13]. Sam-

* Corresponding author.
E-mail address: rdoerner@ucsd.edu (R.P. Doerner).
[1] Present address: Princeton Plasma Physics Laboratory, Princeton, N.J., 08540 USA.

http://dx.doi.org/10.1016/j.nme.2016.09.002

ple temperature is monitored by a thermocouple pressed firmly against the back surface of the sample and the temperature during exposure is controlled by varying the coolant flow through the sample manipulator. Plasma conditions are measured using a reciprocating Langmuir probe.

The first set of experiments compared sequential helium then deuterium plasma exposure to simultaneous D/x%He plasma where the helium ion content, x, was varied from 5 to 10%. These experiments used standard ^{4}He gas to generate the helium plasma ions. Nuclear reaction analysis (NRA) using the D(^{3}He,p)^{4}He reaction was applied under perpendicular angle of incidence to determine the deuterium content retained in the exposed samples as outlined in [14]. Protons were detected with different ^{3}He energies between 0.5 and 4.5 MeV with a thick surface barrier PIPS detectors (detector 1 with a solid angle of 29.2 msr and detector 2 with a solid angle of 72.1 msr) under 135° scattering angle in the center of the samples. In order to improve depth resolution near the surface α particles were energy analyzed with a surface barrier detector at a laboratory scattering angle of 102° equipped with a slit reducing the solid angle to 9.2 msr. The samples then underwent thermal desorption spectrometry (TDS) in an attempt to remove the retained deuterium. The sample temperatures were ramped to 1273 K in a quartz tube using radiant heaters at a linear rate of 0.3 K/s and held at 1273 K for 900 s before cooling. A high-resolution MKS residual gas analyzer capable of resolving the difference in release between D_2 molecules and helium atoms was used. Finally, the samples were once again subjected to NRA to quantify the amount of deuterium remaining trapped in the tungsten. Elastic recoil detection analysis (ERDA) using an 15 MeV oxygen ion beam as described in [15] was also used on the samples before and after TDS to monitor any reduction in the helium content in the samples due to the heating cycle.

The drawback of ERDA measurements is the difficulty to accurately quantify the total amount of helium on rough surfaces because of the grazing angle of incidence. For this reason a second set of samples were exposed to pure helium plasma consisting of a mixture of ^{3}He (25%) and ^{4}He (75%). The mixed He gas cylinder was supplied by Linde Industrial Gases. Due to the cost of ^{3}He, the pumping system of the PISCES-A device had to be modified to limit the gas throughput during the plasma exposure. Two turbomolecular pumps (1800 l/s and 1300 l/s) are used to pump the PISCES-A chamber. Typically, one of these pumps is closed during plasma operation, but both can remain open, depending on the plasma parameters desired. In the case of the ^{3}He plasma, a separate throttled (300 l/s) turbomolecular pump is used while the two large pumps are both closed. Even with the smaller throughput, no evidence of impurity accumulation during the plasma exposure was observed. For these experiments, tungsten samples (25 mm diameter, 1 mm thick disks) are used. These tungsten samples are also ITER grade, but made by Midwest Tungsten Service, Inc. via powder metallurgy by press-sintering 99.95 wt% pure tungsten powder. The tungsten grains are also elongated in the direction normal to the surface.

The samples that were exposed to ^{3}He plasma at different fluences and temperatures were then analyzed using a high energy deuterium ion beam to generate the ^{3}He(D,^{4}He)p nuclear reaction. Protons were also detected with a thick PIPS detector under 135° scattering angle (solid angle (22 ± 1) msr). During this analysis the ion beam was moved across the diameter of the sample in a series of steps to check for uniformity across the sample surface. Since ^{3}He made up only 25% of the He ions in the plasma, the measurements of ^{3}He in the samples has been multiplied by four to obtain the total quantity of helium retained.

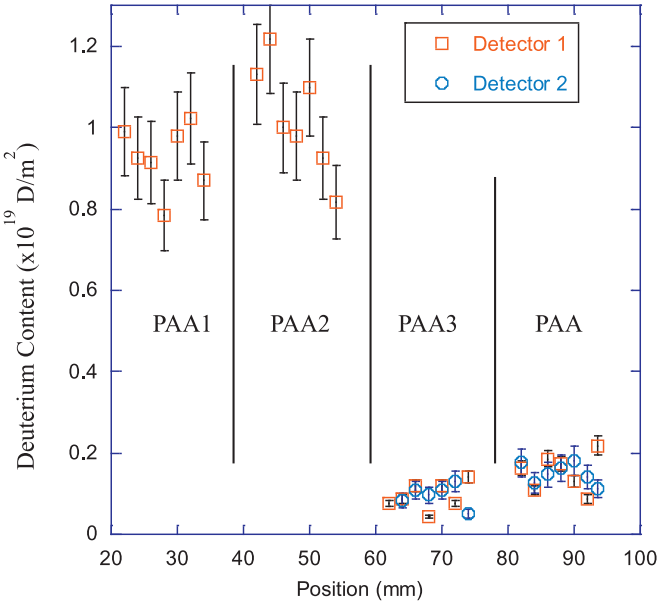

Fig. 1. Deuterium content in samples exposed to simultaneous D/He plasma (PAA1 with 5% He, PAA2 with 10% He) and sequential He then D plasma (PAA3 at 573 K and PAA4 at 773 K).

3. Results and discussion

3.1. D-He interactions in w

The goal of the first set of measurements, involving deuterium retention, was to determine whether all the deuterium in the samples is released during TDS to 1273 K. Recent atomistic modeling has seen evidence of D partitioning in W to regions near the edges of He filled bubbles and that D atoms residing at these locations are stable at temperatures exceeding those available using our TDS system [16]. While the TDS measurements cannot determine where the D is located in the sample, it can be used to verify the predicted energy level of the traps.

Two tungsten samples were exposed to mixed D/He plasma with either 5 or 10% ^{4}He ion composition of the plasma. These samples were exposed to a total fluence of 1×10^{26} m^{-2}, at 523 K with an incident ion energy of 40 eV Two additional tungsten samples were exposed to sequential helium and then deuterium plasma, one sample was exposed at 573 K, the other at 773 K. Both of these samples were exposed to a ^{4}He fluence of 1×10^{25} m^{-2} and a deuterium fluence of 1×10^{26} m^{-2}, again with 40 eV incident ion energy. Table 1 summarizes the exposure conditions of all samples. The deuterium content measured across the face of each of these samples and is shown in Fig. 1. The measurement is made with a 800 keV ^{3}He ion beam and the energy spectra of the protons is collected in the two thick PIPS detectors simultaneously. For each data point a total charge of 10 μC of ^{3}He was collected within a beam spot of 1×1 mm^2. The alpha signal was used to check for the D depth distribution. Because Fig. 1 shows a homogenous distribution and to enhance sensitivity all alpha spectra collected across the face of the individual samples were summed and compared with SIMNRA [17] and ResolNRA [18] calculations. The measured spectra for the simultaneously exposed samples are simulated best when all D is assumed to be in a surface layer whose width is determined by the depth resolution of 170×10^{19} W/m^2. Assuming W bulk density, this converts to a thickness of 26 nm and hence the majority of the D resides within the 20–30 nm thick ^{4}He nano-bubble layer. The experimental data and simulation fits assuming various D depth distributions are shown in Fig. 2. The

Please cite this article as: R.P. Doerner et al., Quantitatively measuring the influence of helium in plasma-exposed tungsten, Nuclear Materials and Energy (2016), http://dx.doi.org/10.1016/j.nme.2016.09.002

Table 1
Sample exposure conditions for all targets used in this study.

Sample	Plasma composition	Ion flux ($m^{-2}s^{-1}$)	Fluence (m^{-2})	Temperature (K)	Ion energy (eV)	Exposure time (s)
PAA1	D_2/5%He	1.1×10^{22}	1×10^{26}	523	40	9300
PAA2	D_2/10%He	7.8×10^{21}	1×10^{26}	523	40	12,840
PAA3	He (first exposure)	2.0×10^{22}	1×10^{25}	573	40	500
PAA3	D_2 (second exposure)	4.1×10^{21}	1×10^{26}	573	40	23,820
PAA4	He (first exposure)	3.0×10^{22}	1×10^{25}	773	40	334
PAA4	D_2 (second exposure)	1.2×10^{22}	1×10^{26}	773	40	8340
He3-1	25%^{3}He/75%^{4}He	2.7×10^{22}	2.5×10^{25}	773	70	930
He3-2	25%^{3}He/75%^{4}He	3.2×10^{22}	2.0×10^{26}	773	70	6250
He3-3	25%^{3}He/75%^{4}He	8.0×10^{22}	3.0×10^{26}	1173	70	3750
He3-4	25%^{3}He/75%^{4}He	2.0×10^{22}	2.5×10^{25}	973	70	1250

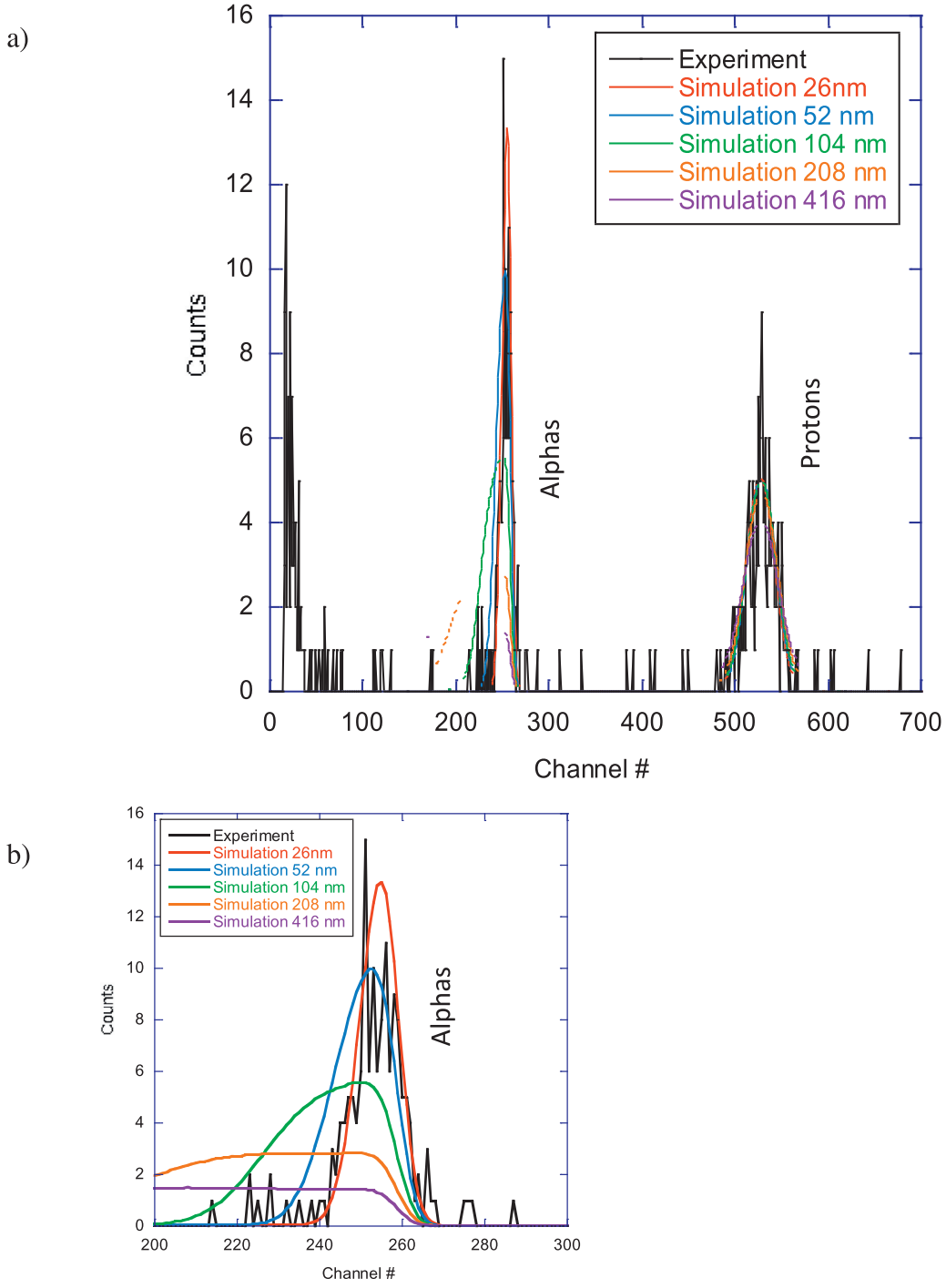

Fig. 2. Comparison of the measured full NRA spectrum (a) from sample PAA2 with simulated spectra assuming various deuterium depth profiles, b) expands the alpha signal and fits for clarity.

Please cite this article as: R.P. Doerner et al., Quantitatively measuring the influence of helium in plasma-exposed tungsten, Nuclear Materials and Energy (2016), http://dx.doi.org/10.1016/j.nme.2016.09.002

magnitude of the retention is consistent with previous mixed D/He retention measurements [19 and references therein] and would tend to confirm the atomistic modeling prediction of D partitioning to the regions near the He bubbles [16]. One can also see the retention in the sequentially exposed samples is much less than in the samples exposed to simultaneous D and ^{4}He bombardment. In the case of the sequential exposures, the helium nano-bubbles are fully formed before the onset of deuterium ion irradiation and so the uptake is inhibited from the initiation of the deuterium plasma. In the sequentially exposed samples, the NRA signals are too small to get an accurate depth distribution of the D.

The integrated deuterium release during the TDS was measured to be 1.5×10^{19} D/m^2 for the sample exposed to 5% ^{4}He plasma and 0.7×10^{19} D/m^2 for the sample exposed to 10% ^{4}He plasma. Due to the low signal levels of D released from the samples, an error approaching 50% is associated with the TDS measurements. Despite this large uncertainty, the desorption results are consistent with the majority of the D in the samples being trapped in the nano-bubble layer. The integrated release is also consistent with all the deuterium being released by the maximum oven temperature of 1273 K. The deuterium release during the TDS of the sequentially exposed samples was below the system's limit of detection.

For completeness, NRA was again performed on each of the samples following TDS, but no measureable deuterium was found to remain in the samples. The limit of detection for the NRA measurements was 3×10^{17} D/m^2. The fact that all the deuterium is released during TDS is in contradiction with expectations from molecular dynamics modeling [16]. However, the timescales associated with MD modeling (picoseconds to nanoseconds) is drastically different from those encountered during the experiments (hours). Another uncertainty lies in the potentials used, as the behavior of H and He in the simulations are quite sensitive to the details of these potentials [20]. In spite of these uncertainties, it is clear that deuterium neither remains trapped in the tungsten, nor in molecular form in the bubbles, after the heating cycle and that, therefore, a significant molecular deuterium concentration within the bubbles during the plasma exposure is unlikely.

ERDA using an 15 MeV oxygen ion beam under a scattering angle of 30° was also applied before and after TDS to determine the relative amount of helium released during the temperature ramp. Quantification of the amount of helium in the samples was difficult, but the reduction of the raw count rates easily gives the relative amount of helium remaining in the samples. Different release behavior was observed from the sequentially and simultaneously exposed samples. The simultaneously exposed samples, lost 67% of the helium retained during the plasma exposure, whereas the sequentially exposed samples lost only 23% of their retained helium. This surprising result clearly indicates that more work will be needed to understand the complex interaction between deuterium and helium in tungsten.

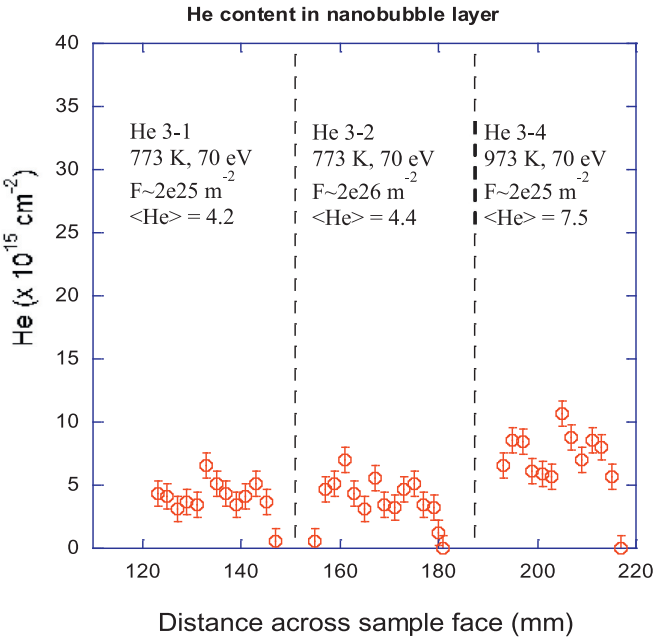

Fig. 3. Comparison of helium content in samples exposed at different fluence (He3-1 and He3-2) and different temperature (He3-1 and He3-4).

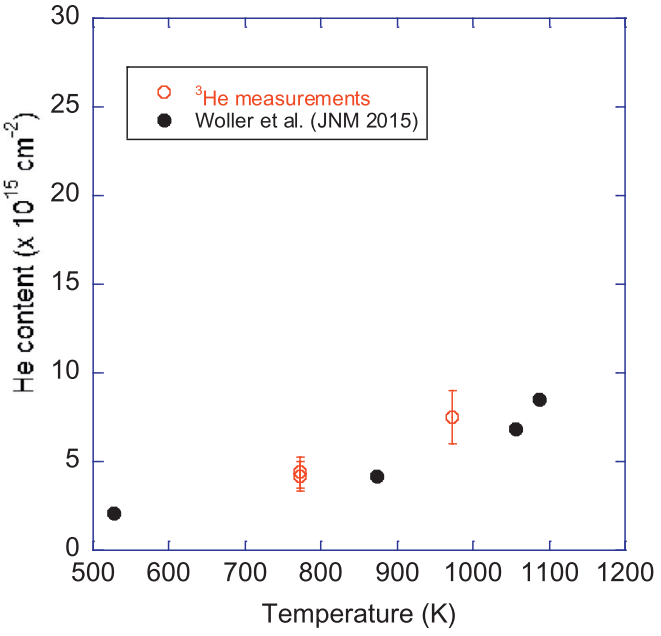

Fig. 4. Helium content in tungsten samples as a function of the temperature during plasma exposure. No fuzz formed on these surfaces.

3.2. Quantification of He in w

A second set of measurements were made on tungsten samples exposed to pure He plasma consisting of 25% ^{3}He and 75% ^{4}He. The goal of these measurements was to begin to understand the sub-surface nano-bubble layer formation at different fluences and temperatures. First, two samples were exposed at 773 K to different fluences, namely 2×10^{25} m^{-2} and 2×10^{26} m^{-2}, at 70 eV ion energy. A third sample was exposed to a fluence of 2×10^{25} m^{-2} and 70 eV, but at 973 K. The results showing the absolute number of He atoms in the nano-bubble layer are shown in Figure 3. Here we assume that the behavior of ^{3}He and ^{4}He in the plasma and in the material is similar and have multiplied the measured ^{3}He by a factor of four to account for the fill gas composition. The helium content in the bubble layer does not change with increasing fluence and increases only slightly with the increase in temperature.

It has also been shown that the thickness of the nano-bubble layer saturates with increasing He fluence at about 20–30 nm thickness and contains bubbles with roughly a 1–2 nm diameter [21]. Finally, the density of He bubbles has also been measured [22] and saturates at a value of about 1.3×10^{17} m^{-2} at 773 K. These values can be used to estimate the number of He atoms/bubble and the pressure in the bubbles. Simply dividing the measured helium content (4.3×10^{19} m^{-2} at 773 K from Fig. 3) by the bubble density gives approximately 330 He/bubble. Similarly, the number of missing W atoms in a bubble of 1.5 nm diameter is about 110.

Please cite this article as: R.P. Doerner et al., Quantitatively measuring the influence of helium in plasma-exposed tungsten, Nuclear Materials and Energy (2016), http://dx.doi.org/10.1016/j.nme.2016.09.002

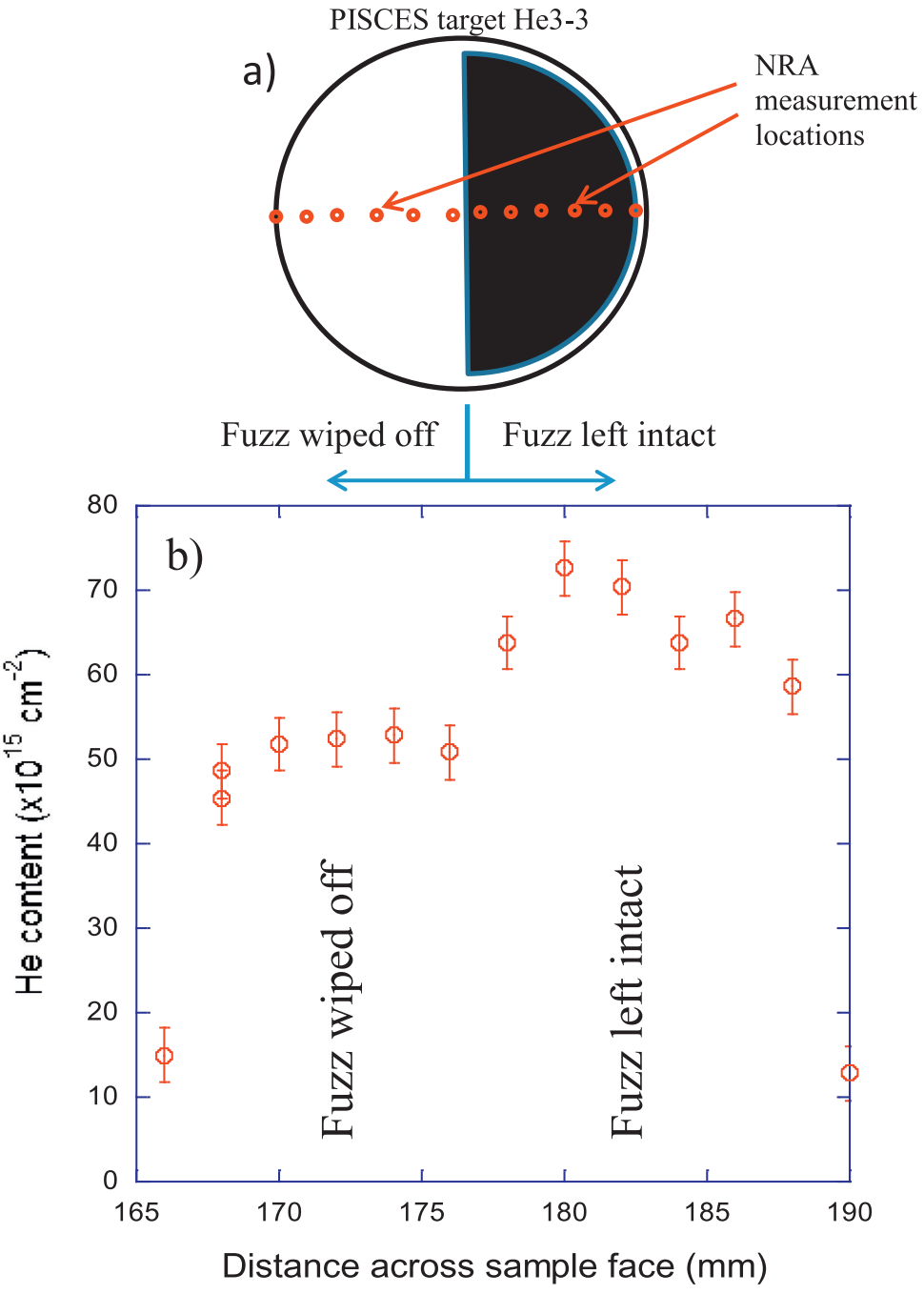

Fig. 5. Measurements were made on a fuzzy tungsten sample where (a) half the fuzz has been wiped off the surface, (b) resulting helium content in regions with and without fuzz.

This gives us a value of about 3 He/vacancy in the bubbles, which is similar to the values used in modeling [16].

These measurements of helium concentration in tungsten can be compared with recent ERDA measurements made during plasma exposure in DIONISIS [23]. The absolute helium concentration measured in all the samples are plotted in Fig. 4. The agreement between the two methods is very good and a small increase in helium concentration with increasing temperature is also observable. It should also be noted that the helium fluence in [23] is one to two orders of magnitude less than in the ^{3}He samples. This confirms the fact that the helium bubble layer readily forms and quickly saturates with increasing fluence. Assuming that the bubble layer in these samples is 25 nm thick, the value for He/W in this region is about 3%, again in good agreement with [23].

A final sample was exposed to ^{3}He at 1173 K (a temperature sufficient for fuzz to form) to a fluence of 3×10^{26} m^{-2} and 50 eV. This sample provided the opportunity to measure the helium content in the fuzz tendrils. After the fuzzy sample was removed from PISCES-A, the mass of the sample was measured before and after wiping the fuzz off one half of the sample surface with a cotton swab. The mass of the removed fuzz structures was 96 ± 10 µg, or 3.1×10^{17} W atoms. NRA was then measured at several points across the samples surface spanning the clean half to the fuzzy half of the sample, as depicted in Fig. 5a. Fig. 5b shows the He content in the sample with and without the fuzz on the surface. The

Please cite this article as: R.P. Doerner et al., Quantitatively measuring the influence of helium in plasma-exposed tungsten, Nuclear Materials and Energy (2016), http://dx.doi.org/10.1016/j.nme.2016.09.002

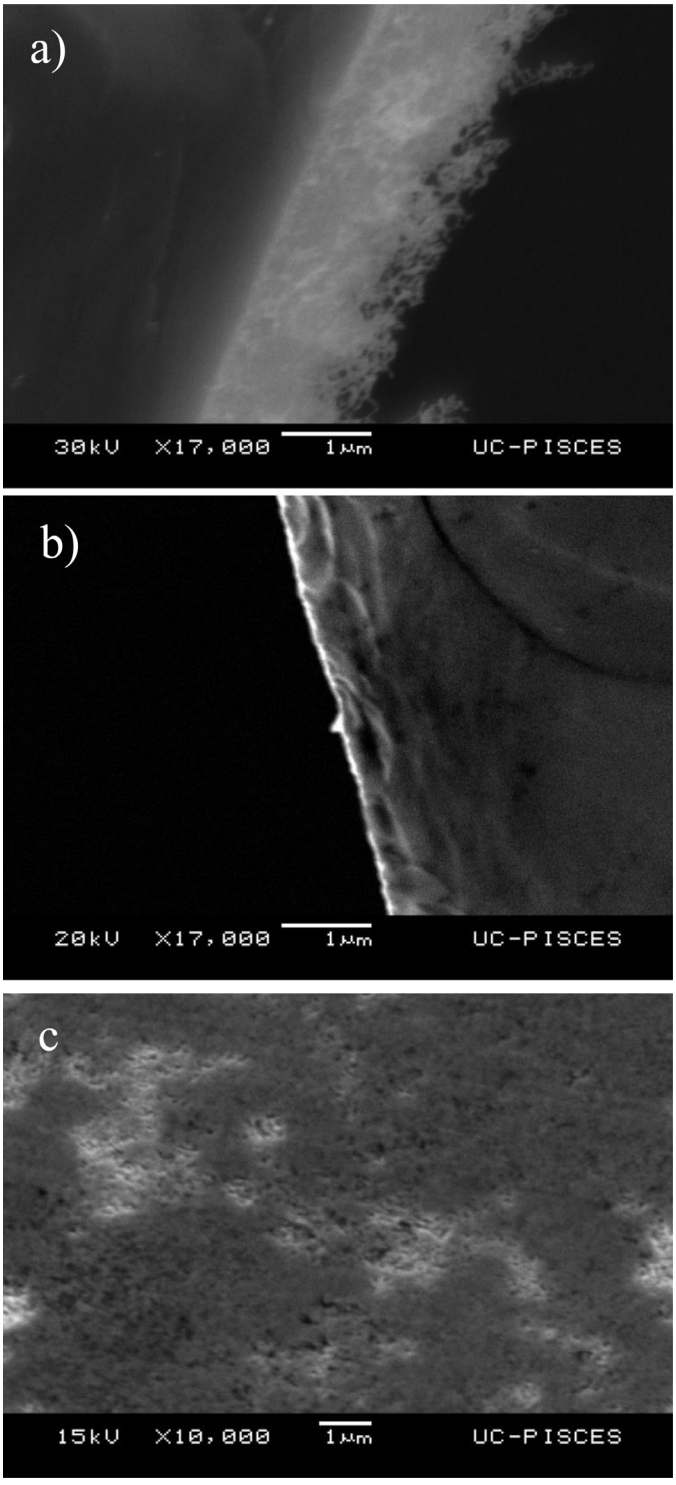

Fig. 6. Edge SEM view of a fuzzy tungsten surface (a) before and (b) after fuzz has been wiped off the surface. Surface view of surface after fuzz removal showing only larger base structures of the fuzz remain.

amount of helium missing from the side with the fuzz removed is approximately 16×10^{19} He/m^2, or a total of 3×10^{16} He atoms. This results in an average value for the He/W ratio in the fuzz of about $10 \pm 2\%$. This value is in good agreement with [23] and a more recent measurement [24].

The other striking aspect of Fig. 5b is the fact that the majority of the helium remains in the sample, below the surface from which the fuzz has been removed. Edge SEM views of the fractured sample with, and without, the fuzz layer removed are shown in Fig. 6. To the eye the sample with the fuzz removed returns to a smooth metallic appearance, SEM images confirm the cotton swab was effective in removing the thin fuzz tendrils, while leaving some evidence of the larger base structures of the fuzz intact, implying that the remaining helium is located in the base of the structures, or below the surface. This is consistent with TEM images of fuzzy structures showing a region of dense, but larger bubbles located just below the surface in the fuzzy samples [25–27]. Such a region of high He concentration could create a layer of high stress and be the 'growth plate' which causes the deformation of the surface and results in fuzz growth.

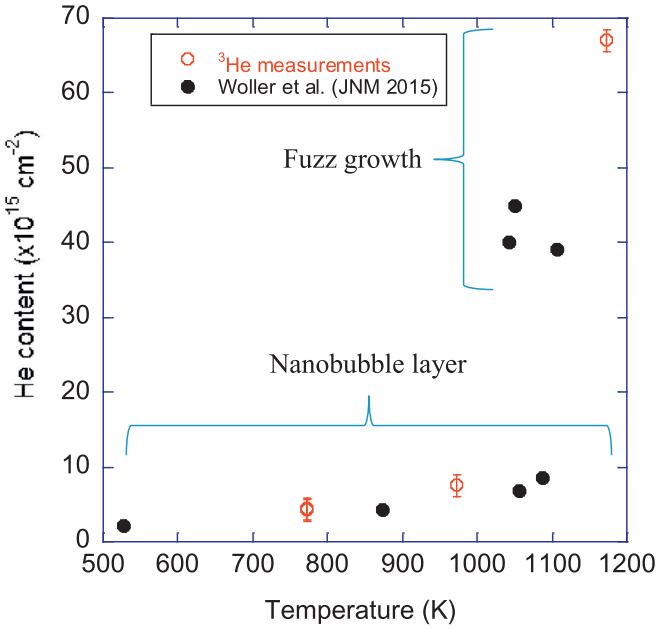

Fig. 7. Helium content with changing surface temperature, indicating an increase in helium when fuzz grows on the surface.

Finally, it is interesting to include the He content data points for the fuzzy samples from [23] and this work with the data already shown in Fig. 4. All the helium concentration data points are plotted in Fig. 7 as a function of the sample temperature during plasma exposure. A dramatic increase in helium content is seen in all the fuzzy samples, compared to the samples which did not grow fuzz. Remarkably, some of the samples measured in [23] were at sufficient temperature to allow fuzz growth, but had not yet achieved the incubation fluence of 2.5×10^{24} m^{-2} [28] necessary for the fuzzy structure to form. These samples are seen to have much less helium content than the samples with fully developed fuzzy structures.

4. Summary

A series of measurements were made on tungsten samples exposed to mixtures of helium and deuterium plasma in support of atomistic modeling activities. Retained deuterium and helium were measured both before and after thermal desorption (to 1273 K) mass spectrometry of tungsten samples exposed to both sequential and simultaneous D/He plasma. Measurements show the majority of the D retained during simultaneous exposures is located in the near surface region of helium nano-bubbles. In all cases, no deuterium was detected after the single heating cycle. Of the helium retained in the samples, 67% was released from simultaneously exposed samples, but only 23% of the helium was released from the sequentially exposed samples. Tungsten samples

Please cite this article as: R.P. Doerner et al., Quantitatively measuring the influence of helium in plasma-exposed tungsten, Nuclear Materials and Energy (2016), http://dx.doi.org/10.1016/j.nme.2016.09.002

were also exposed to ^{3}He plasma to provide a quantitative measure of the helium retained during plasma exposure. The thin helium nano-bubble layer contained 4.3×10^{19} He/m^2 at 773 K, independent of the plasma fluence and this value increased slightly to 7.5×10^{19} He/m^2 for 973 K exposure. The helium content increased dramatically to 6.8×10^{20} He/m^2 when fuzz formed on the surface of a sample exposed at 1173 K, but the majority of the retained helium (5.1×10^{20} He/m^2) was found to reside below the layer of fuzz tendrils.

Acknowledgments

This work was supported by a grant from the Department of Energy, DE-FG02-07ER54912, and as part of the US-EU Bilateral Collaboration on Mixed Materials for ITER.

References

[1] M.J. Baldwin, et al., J. Nucl. Mater. 415 (2011) S104.
[2] M. Miyamoto, et al., J. Nucl. Mater. 415 (2011) S659.
[3] M. Thompson, et al., Nucl. Fusion 55 (2015) 042001.
[4] S. Takamura, et al., Plasma Fusion Res 1 (2006) 51.
[5] M.J. Baldwin, et al., Nucl. Fusion 48 (2008) 035001.
[6] D. Nishijima, et al., J. Nucl. Mater 329-333 (2004) 1029.
[7] S. Kajita, et al., Nucl. Fusion 49 (2009) 095005.
[8] K.O.E. Hendersson, et al., Appl. Phys. Lett. 87 (2005) 163113.
[9] G-H. Lu, et al., Nucl. Fusion 54 (2014) 086001.
[10] B.D. Wirth, et al., J. Nucl. Mater. 463 (2015) 30.
[11] D.M. Goebel, et al., J. Nucl. Mater. 145-147 (1987) 61.
[12] Material Specification for the Supply of Tungsten Bars for the ITER Divertor IDM Number: ITER_D_2X38PN – v. 1.0, 2010.
[13] D. Nishijima, et al., Phys. Plasmas 14 (2007) 103509.
[14] M. Mayer, et al., Nucl. Instrum. Methods B 267 (2009) 506.
[15] E. Markina, et al., Nucl. Instrum. Methods B 269 (2011) 3094.
[16] N. Juslin, B.D. Wirth, J. Nucl. Mater. 438 (2013) S1221.
[17] M. Mayer, SIMNRA User's Guide, Max-Planck-Institut für Plasmaphysik, Garching, Germany, 1997 Report IPP 9/113.
[18] M. Mayer, Nucl. Instrum. Methods B 266 (2008) 1852.
[19] M.J. Baldwin, et al., Nucl. Fusion 51 (2011) 103021.
[20] M. Cusention, et al., J. Nucl. Mater. 463 (2015) 347.
[21] R.P. Doerner, et al., Phys. Scr. T167 (2016) 014054.
[22] M. Miyamoto, et al., Phys. Scr. T159 (2014) 014028.
[23] K.B. Woller, et al., J. Nucl. Mater. 463 (2015) 289.
[24] Yu. Gasparyan, et al., Nucl. Fusion 56 (2016) 054002.
[25] S. Kajita, et al., J. Nucl. Mater. 418 (2011) 152.
[26] A. Khan, et al., J. Nucl. Mater. 474 (2016) 99.
[27] C. Parish, et al., The microstructure of plasma-expsoed tungsten and tungsten nanotendrils, presented at the 22nd International Conference on Plasma-Surface Interactions in Controlled Fusion Devices, 2016.
[28] T.J. Petty, et al., Nucl. Fusion 55 (2015) 093033.

Please cite this article as: R.P. Doerner et al., Quantitatively measuring the influence of helium in plasma-exposed tungsten, Nuclear Materials and Energy (2016), http://dx.doi.org/10.1016/j.nme.2016.09.002